New Northern Snowpack Classification Linked to Vegetation Cover on a Latitudinal Mega-Transect Across Northeastern Canada

Authors: Royer, Alain, Domine, Florent, Roy, Alexandre, Langlois, Alexandre, Marchand, Nicolas, et al.

Taylor & Francis
Taylor & Francis Group

New northern snowpack classification linked to vegetation cover on a latitudinal mega-transect across northeastern Canada

Alain Royer[a,b], Florent Domine[b,c,d], Alexandre Roy[b,e], Alexandre Langlois[a,b], Nicolas Marchand[a] and Gautier Davesne[b,f]

[a]Centre d'applications et de recherche en télédétection (CARTEL, Université de Sherbrooke, Sherbrooke, Québec, Canada; [b]Centre d'études nordiques, Québec, Canada; [c]Takuvik Joint International Laboratory, Université Laval (Canada) and CNRS-INSU (France), Quebec City, Québec, Canada; [d]Department of Chemistry, Université Laval, Quebec City, Québec, Canada; [e]Département des Sciences de l'environnement, Université du Québec à Trois-Rivières, Trois-Rivières, Canada; [f]Department of Geography, Université de Montréal, Montréal, Québec, Canada

ABSTRACT

Changes in mass, extent, duration, and physical properties of snow are key elements for studying associated climate change feedbacks in northern regions. In this study, we analyzed snowpack physical properties along a 'mega' transect from 47°N to 83°N (4,000 km) in northeastern Canada, which includes marked transitions between ecozones from boreal forest to subarctic and arctic ecosystems. Our unique dataset of 391 detailed snowpits acquired over the last 20 years, complemented with snow data from weather stations, shows that snowpack properties such as snow water equivalent, snow depth, density, grain size and basal depth hoar fraction (DHF) are strongly linked to vegetation type. Based on these results, we propose an updated classification of snow types in three classes: boreal forest snow (47–58°N), tundra snow (58–74°N) and polar desert snow (74–83°N), which is more appropriate to the study area than the general north hemisphere classification commonly used. We also show that shrub presence along the transect contributes to a significant increase in DHF development which contributes most strongly to the thermal insulation properties of the snowpack. Overall, our analysis suggests that snow–vegetation interactions have a positive feedback effect on warming at northern latitudes.

RÉSUMÉ

Les changements dans la masse, l'étendue, la durée et les propriétés physiques du manteau neigeux sont des éléments clés pour l'étude des rétroactions du changement climatique dans les environnements nordiques. Dans cette étude, nous avons analysé les propriétés physiques du couvert nival le long d'un « méga » transect de 47°N à 83°N (4000 km) dans le nord-est du Canada, comprenant des transitions marquées entre l'écozone de la forêt boréale et les écosystèmes subarctiques et arctiques. Notre ensemble de données uniques de 391 puits de neige détaillés, acquis au cours des 20 dernières années, enrichi de données de neige provenant de stations météorologiques, montre que les propriétés du manteau neigeux telles que l'équivalent en eau de la neige (EEN), l'épaisseur de la neige, la densité, la taille des grains et la fraction de la couche de givre de profondeur sont fortement liées aux types de végétation. Ces résultats nous mènent à proposer une classification actualisée des types de neige en trois classes: neige de forêt boréale (47–58°N), neige de toundra (58–74°N) et neige de désert polaire (74–83°N), qui est plus appropriée à la région étudiée que la classification globale de l'hémisphère nord généralement utilisée. Nous mettons également en évidence que la présence d'arbustes le long du transect contribue à une augmentation significative du développement de la couche basale du givre de profondeur. Globalement, notre analyse suggère que les interactions neige-végétation rétroagissent positivement sur le réchauffement nordique.

Introduction

Snow usually covers the ground for more than half of the year in northern regions, making it a key environmental component. Snow is a medium where many physical variables interact with climate (temperature, precipitation, wind) and with the soil and vegetation (Pearson et al. 2013; Meredith et al. 2019; Diro and Sushama 2020; Grünberg et al. 2020). Past analyses of snow time series have mainly focused on snow cover duration and extent (Brown and Mote 2009; Brown et al. 2010; Liston and Hiemstra 2011; Mortimer et al. 2020), and on snow water equivalent (SWE) (Takala et al. 2011; Larue et al. 2017) or snow mass (SWE x Snow Extent) (Pulliainen et al. 2020). Specifically, Pulliainen et al. (2020) showed that, over the last 40 years, snow mass has decreased by 4% per decade across North America,

but that no such trend was detected in Eurasia. Both continents exhibit high regional variability, mainly driven by variable regional warming and precipitation rates. The positive feedback effects of increased snowfall can counter the negative feedback effect of warming on SWE (Brown and Mote 2009). Also, topography and vegetation contribute to local variability by affecting snow accumulation. However, while variables impacting SWE and snow cover duration have been investigated, few studies have analyzed how the physical properties of the snowpack are linked to regional and local spatial variability.

Snowpack properties, mainly density, thermal conductivity and microstructure (snow grain type), govern heat exchanges between the atmosphere and the ground through the snow, and therefore soil temperature (Park et al. 2015; Domine et al. 2019). In turn, soil temperature affects the temperature gradient in the snowpack and therefore the conditions of snow metamorphism that may lead to the formation of large snow crystals known as depth hoar, mostly at the base of the snowpack (Colbeck 1993; Sturm and Benson 1997; Domine et al. 2016b). Depth hoar layers form under large temperature gradients that drive large upward water vapor fluxes. These layers are responsible for most of the thermal insulation properties of snowpacks in the Arctic (Zhang et al. 1996). The temperature gradient, especially at the beginning of the snow season, is affected by soil moisture, as greater moisture maintains the soil at 0°C for a longer period, allowing for large temperature gradients to persist and favoring depth hoar formation (Domine et al. 2018). Wind also strongly affects snow thermal properties. Snow drifting during the windy episodes that frequently sweep barren Arctic regions leads to the formation of hard dense wind slabs with a high thermal conductivity that favor soil cooling, reduce the temperature gradient in the snowpack and limit or prevent depth hoar formation (Domine et al. 2018). Lastly, snow depth, largely determined by the amount of snowfall, also determines snow physical properties.

Vegetation characteristics also affect snow properties. For example, boreal forests essentially prevent wind drifting, while shrubs affect snowpack properties by not only enhancing snow depth and SWE through a trapping effect further north (e.g., Sturm et al. 2001; Marsh et al. 2010; Paradis et al. 2016; Busseau et al. 2017) but also increasing the formation of depth hoar within shrubs (Sturm et al. 2001; Domine et al. 2016a; Gouttevin et al. 2018). The challenge here is to know if, in general, both effects lead to more insulation by snow changing and therefore to ground warming.

Climate change generates modifications in air temperature and precipitation regimes, but it also leads to changes in vegetation and soil moisture (Tape et al. 2006; Myers-Smith et al. 2011; Callaghan et al. 2011; Xu et al. 2013; Ju and Masek 2016; Martin et al. 2017). These induced changes are also important factors influencing key snowpack characteristics (Lawrence and Slater 2010; AMAP 2019). Complex snow and land surface processes and feedbacks are not well accounted for in climate models and are an important source of uncertainty in inferring future northern climates (Lawrence and Slater 2010; Dutra et al. 2012; Gouttevin et al. 2012; Chadburn et al. 2015; Paquin and Sushama 2015; Bokhorst et al. 2016; Barrere et al. 2017; Domine et al. 2019; Meredith et al. 2019).

Our objective was to characterize the different snow types based on their physical properties observed along a 4,000 km transect from 47°N to 83°N in northeastern Canada. We explore the relationship between climate, vegetation and snow physical properties over this uniquely large climate and vegetation gradient from boreal forest to Arctic tundra and polar desert. Our findings may guide future climate models to better integrate snow-vegetation-climate feedbacks. Our study exploits a unique and outstanding dataset of detailed in-situ snowpit measurements acquired by our groups over the last 20 years. Our analysis of snowpack properties leads to a new snow classification, better adapted to the specificities of northeastern Canada, and which differs from Sturm et al.'s (1995) more general snow classification.

Study area and datasets

Study area

The transect over northeastern Canada extends between 47°N and 83°N and between 65°W and 80°W in its southern part, and shifts slightly to 70°W–90°W in its northern part (Figure 1). Figure 1(a) shows the distribution of the study sites where in-situ field campaigns occurred (Table 1) and where meteorological station data are available. The permafrost zones, given as complementary information, are also shown (Figure 1(a)). The gradient of vegetation cover along the transect is displayed in Figure 1(b) with highlighted tree line at 58.5° (orange line) (Payette et al. 2001). The vegetation zones spanning from closed boreal forest to High Arctic polar desert were simplified into eight classes, from south to north: (1) Eastern sub-boreal mixed forest, with a coniferous dominance; (2) Closed-crown coniferous boreal forest; (3) Open-crown coniferous boreal forest, e.g., lichen woodland; (4) Forest tundra;
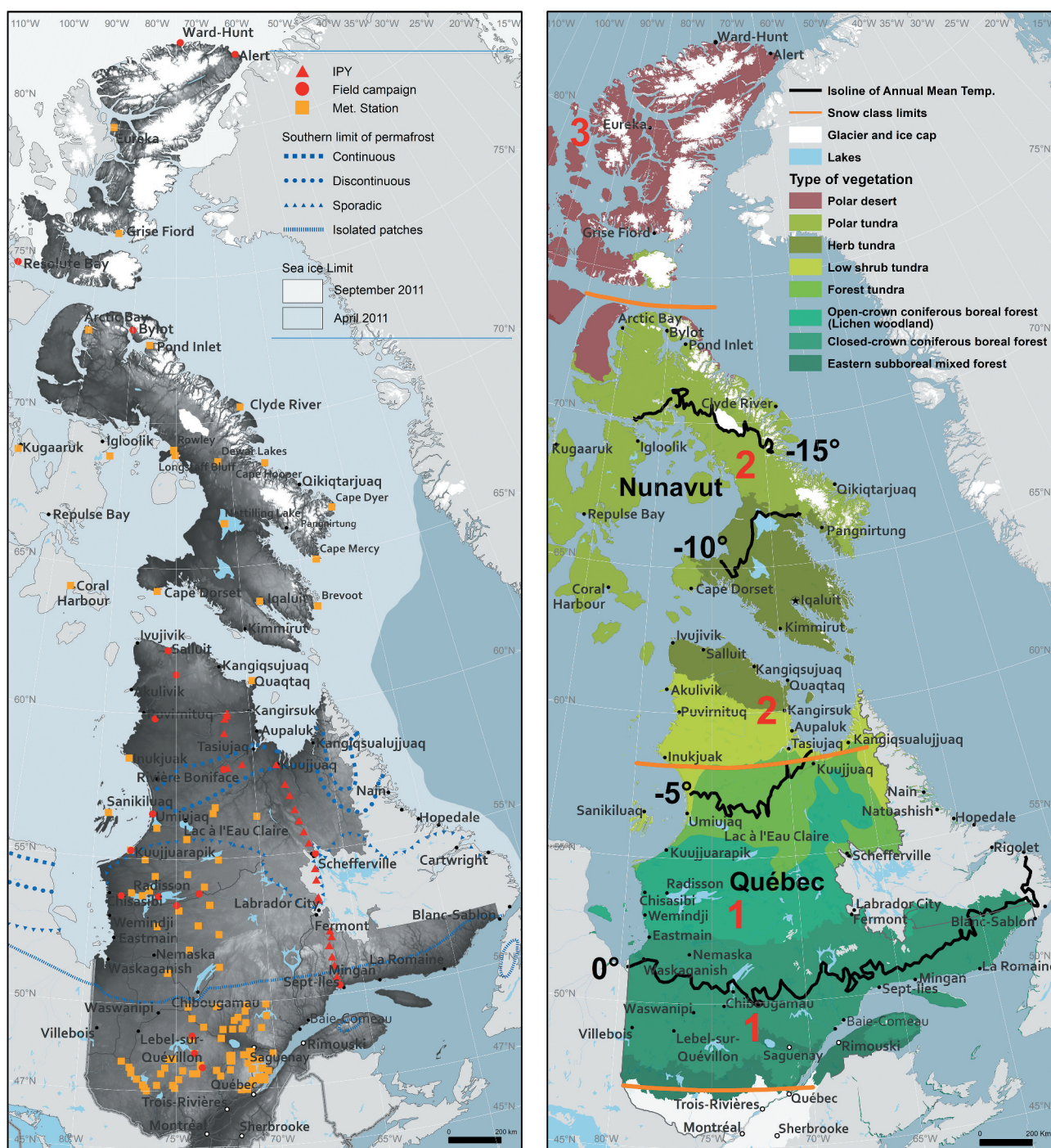
Figure 1. Left: Locations of in-situ field campaigns and meteorological stations used across the area studied in northeastern Canada between 47°N and 83°N. The background image corresponds to the topography, with mean altitude values ranging from 0 to 900 m a. s.l., no studied sites are in mountain areas. Black points correspond to main northern communities and southern towns. Right: Simplified vegetation cover along the analyzed transect. Black lines correspond to the mean annual air temperature isolines each 5°C from −15 to 0°C. From south to north, the orange lines delimit, respectively, the southern limit of the transect at 47°N, the position of the tree line and the limit of the polar desert zone. They also delimit the proposed three snow classes (numbers 1, 2 and 3) (see the Results section).

(5) Low shrub tundra; (6) Herb tundra; (7) Polar tundra; (8) Polar desert (Figure 1(b)). This simplified classification in eight classes is based on several sources including Payette (1992); Bliss and Matveyeva (1992); Payette et al. (2001); CAVM (2003); Girard et al. (2008); Myers-Smith et al. (2011); Paradis et al. (2016); Payette and Delwaide (2018); and Leboeuf et al. (2018). Note that the 'Herb tundra' class (6) can include ligneous species

Table 1. Description of snow field campaigns, meteorological station datasets and complementary vegetation datasets used. Snow density and depth hoar fraction were derived from snowpits (SP). The number of snowpits per field campaigns is given. See Figure 1(a) for site locations.

Data or site	Acronym	Latitude °N/Longitude °W	Date	No. of SPs	Method	Sources
					Field campaigns	
Forêt Montmorency	FM	47.31/-71.13	03 2015–2018	11	Snowpits	Larue et al. 2018
IPY transect	IPY	50.2–62.3/-65-80 to −70-90	02 2008	25	Snowpits and SWE core	Langlois et al. 2010
Sept-Iles	SI	50.30/-66.28	02 2008	48	Snowpits	Langlois et al. 2010
James Bay	BJ	53.70/-76.05	03 2013–2016	24	Snowpits	Roy et al. 2016; Larue et al. 2018
Schefferville	Shef	54.90/-66.70	02 2008	34	Snowpits	Langlois et al. 2010
Kuujjuarapik	Kupk	55.26/-77.71	03 2013 and 2016	7	Snowpits	This study
Umiujaq	Umi	56.55/-76.50	03 2012, 14, 15 2017	41	Snowpits	Roy et al. 2016; Larue et al. 2018; Domine et al. 2015**
Kuujjuaq	Kuaq	58.06/-71.95	02 2008	26	Snowpits	Langlois et al. 2010
Puvirnituq	Puv	59.83/-76.47	02 2008	160*	SD probe and SWE core	Derksen et al. 2010
Bylot Island	By	73.16/-79.99	05 2014, 2015	30	Snowpits	Domine et al. 2016a, 2016b**, 2018**; Barrere et al. 2017
Resolute	Res	74.75/-94.97	05 2014, 2016, 19	21	Snowpits	This study
Eureka	Eu	80/-84	2012–2020 04–2011	9 49	SWE core (snow surveys) SWE core and Snowpits	ECCC; Saberi et al. 2017
Alert	Al	82.50/-62.35	04 2000	1	Snowpit	Domine et al. 2002; Cabanes et al. 2002
Ward Hunt	WH	83.09/-74.16	05 2016, 06 2019	13	Snowpits	Domine et al. 2018**
					Meteorological datasets	
Hydro-Québec network	-	46–53/-65-80	03 2012–2016	6	SD SR50 and SWE GMON	Larue et al. 2018
Brown et al's database	-	47–80/-65-80 to −70-95	Over 20 years	108	Various	Brown et al. 2019
					Vegetation data	
LAI max	LAI	47–62/-76-70	07–08 1988-2012	-	Global LAnd Surf. Satellite (GLASS) LAI product	Xiao et al. 2016
Crown-Closure	CC	47–62/-76-70	2011	-	Satellite-derived forest attributes	Beaudoin et al. 2017b

*1.7 km transect with one SP each 10 m.
** and additional data used for this study.

such as *Salix arctica, Salix herbacea* or *Salix reticulata*, which are prostrate and therefore have a stature similar to grasses and mosses, with the same effects on snow. For our purpose, the term 'Herb tundra' is thus more descriptive than 'Prostrate dwarf-shrub tundra', a botanically more precise term (CAVM 2003). The isolines of mean annual air temperatures over the last 35 years (1979–2018) are derived from Karger et al. (2017) (black lines in Figure 1(b)).

Mean climatology

The mean daily winter air temperature, from December to the end of March (DJFM), varies from −12°C at 47°N to −35°C at 83°N. Data were averaged over the last 20 years for all stations per degree of latitude, resulting in a meaningful set of data (see Vincent et al. 2015 for data processing) (Figure 2). The observed latitudinal temperature gradient is almost linear with −0.58°C per degree of latitude. The mean annual solid precipitations do not show a regular trend with latitude, but can be grouped into three latitude ranges, with homogeneous values of 255 ± 43 mm of water equivalent (w.e.) for 47°N–50°N, 154 ± 29 mm (w.e.) for 53°N–58°N and 46 ± 19 mm (w.e.) above 64°N (data from Vincent et al. 2015, averaged over the last 20 years) (Figure 2). The observed gradual decrease in snowfall is marked by a significant transition around 65°N, south of Baffin Island, above which the influence of the Continental Arctic air mass is strong throughout the winter with dry northerly winds.

Temporal changes of meteorological variables impacting the snow cover were not investigated in this study. Temperature and precipitation amounts increased along the transect over the period 1948–2012, with the largest increases in warming and precipitation occurring during winter from the 1980s onward, and more significantly in the North (Vincent et al. 2015; Mudryk et al. 2018). However, we did not observe significant trends in hourly mean wind speed over the 1954–2020 period (not shown). The potential role of climate change on the results is addressed in the discussion section.
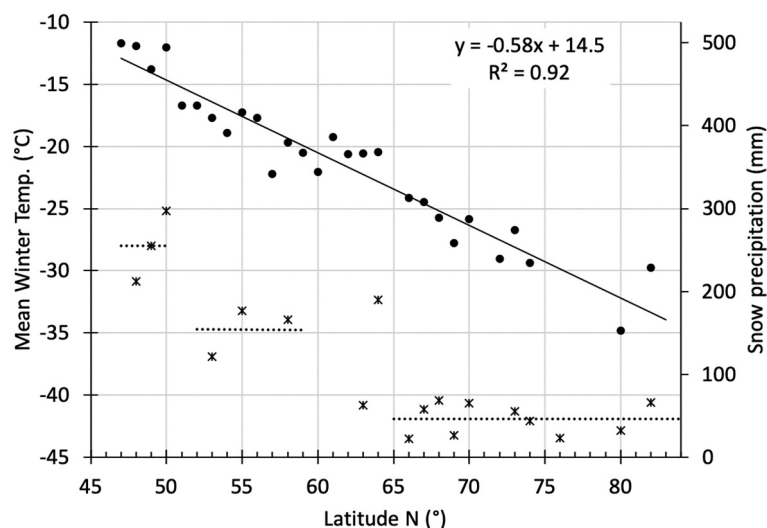
Figure 2. Latitudinal variation of 2000–2019 mean winter air temperatures (DJFM) (dots, left axis) and total snow precipitation (stars, right axis), on a fringe of a few degrees of longitude along the transect. The slope of the temperature linear trend (solid line) is significant: −0.58℃ per degree of latitude. Dotted lines correspond to the relatively homogeneous mean precipitation values per range of latitudes.

Snow data

We gathered a database of 391 snowpits (SP) over the last 20 years, collected during the peak season of snow mass, in March, April or May (Table 1). Snowpit observations consisted of mean snow depth (SD) recorded around the site, density profiles with a vertical resolution of 3 or 5 cm using, respectively, 100 or 250 cm^3 density cutters, a stratigraphy of snow grain types and size based on visually estimated geometric grain size dimensions (following the international classification from Fierz et al. 2009), a temperature profile and ground–snow interface and identification of soil and vegetation types. SWE values (in mm) were derived from vertical density profiles with a mean relative accuracy of 11–12%, assuming an accuracy of the density cutter measurements of about 9% (Proksch et al. 2016).

The ratio of basal depth hoar thickness over snow depth, hereinafter referred to as the depth hoar fraction (DHF), was also considered in this study. When present, the thickness of the depth hoar layer was derived from stratigraphic analysis, grain size measurements, visual identification of grain types and the measurement of specific surface area (SSA) using optical methods (Gallet et al. 2009; Montpetit et al. 2012). The SSA, which corresponds to the grain surface area per unit of mass, is a complementary parameter to geometric grain dimension (Taillandier et al. 2007; Langlois et al. 2020) and both variables can therefore be used to confirm snow classification. The DH SSA is generally lower than 15 m^2 kg^{-1} (Domine et al. 2007, 2018), and its visual grain size is above 2 mm.

To complement the database, an extensive dataset of meteorological station SD and SWE measurements was used (114 samples). Brown et al. (2019) reported the details of these measurements derived from different sources: meteorological stations, automatic measurements and regular (mostly bi-weekly) in-situ surveys using snow cores (such as the Federal Sampler). We only selected data that were recorded near the snow depth maximum date and were then averaged over the last 20 years. In the case of meteorological data, the mean bulk density (ρ) was derived from measured SWE and SD: ρ(kg m^{-3}) = 100 x SWE (kg m^{-2} or mm)/SD (cm).

Table 1 provides detailed information about the data and the sites mapped in Figure 1(a). Data are mostly derived from published research projects, with some additional unpublished data.

Vegetation cover

Vegetation cover zones are mapped in Figure 1(b) in eight classes. The closed-crown boreal forest spans from 47°N to 51°N and the open-crown boreal forest zone extends from 51°N up to 58°N. The open-crown boreal forest (51–58°N) includes the lichen woodland zone in its southern parts (51–55°N) and the forest–tundra ecotone in its northern parts (55–58°N) (Figure 1(b)). These northern boreal forest zones are dominated by mainly black spruce (*Picea mariana*), white spruce (*P. glauca*) and jack pine (*Pinus banksiana*) on generally well-drained soils (Payette and Delwaide 2018). The understory of open-crown forest is mainly composed of lichen (*Cladonia* spp.) and dwarf birch shrubs (*Betula glandulosa)* (Payette and Delwaide 2018). Further north, the tundra zone starts from 58°N

and includes the shrub and herb tundra up until the polar desert is located above 74°N. This study will relate these latitudinal limits, specific to northeastern Canada, to observed snowpack types.

Vegetation was also characterized using two satellite-derived spatially continuous variables (Table 1): (1) Leaf Area Index (LAI) (Xiao et al. 2016) and (2) the percentage of tree cover per surface units, labeled as crown closure (CC) of forest stands (Beaudoin et al. 2017a). The derived LAI values correspond to the summer maximum in vegetation growth at the spatial resolution of 0.05° and to two 10-year averages for two decades: 1988–2000 and 2001–2012. The CC map was derived from images with a spatial resolution of 250 m, using 2011 MODIS satellite data and photo plots from the National Canadian Forest Inventory, and aggregated at 1° latitude intervals along the transect. CC was corrected for water surfaces, and the boundary between open and closed crown forest at 51°N corresponds to closed CC = 25%, in agreement with Girard et al. (2008). Note that the CC database corresponds to a specific period of the survey under study and has certainly evolved since then. It is shown as an example of a continuous latitudinal variation of a quantitative forest parameter, the temporal evolution of the vegetation not being the purpose of this study.

Results

Snowpack and vegetation properties along the transect

We analyzed the latitudinal variations of three main snowpack parameters: SWE, snow depth (SD) and density (ρ). Figure 3 synthesizes all available data along the transect, including field measurements (open symbols, m subscript) and the meteorological dataset (filled symbols, Environment and Climate Change Canada (ECCC) data, EC subscript) (see Table 1 for data description and sources). The values of SWE (top), SD (middle) and density (bottom) are along the transect range, respectively, from 400 to 80 mm, 150 to 20 cm and from 250 to 500 kg m^{-3} (Figure 3). We highlight here the local spatial variability of each parameter by providing values of a standard deviation when a large number of measurements per site (over ~10) were available (vertical bars on SWE, SD and density data, Figure 3). The large value of the observed mean coefficient of variation
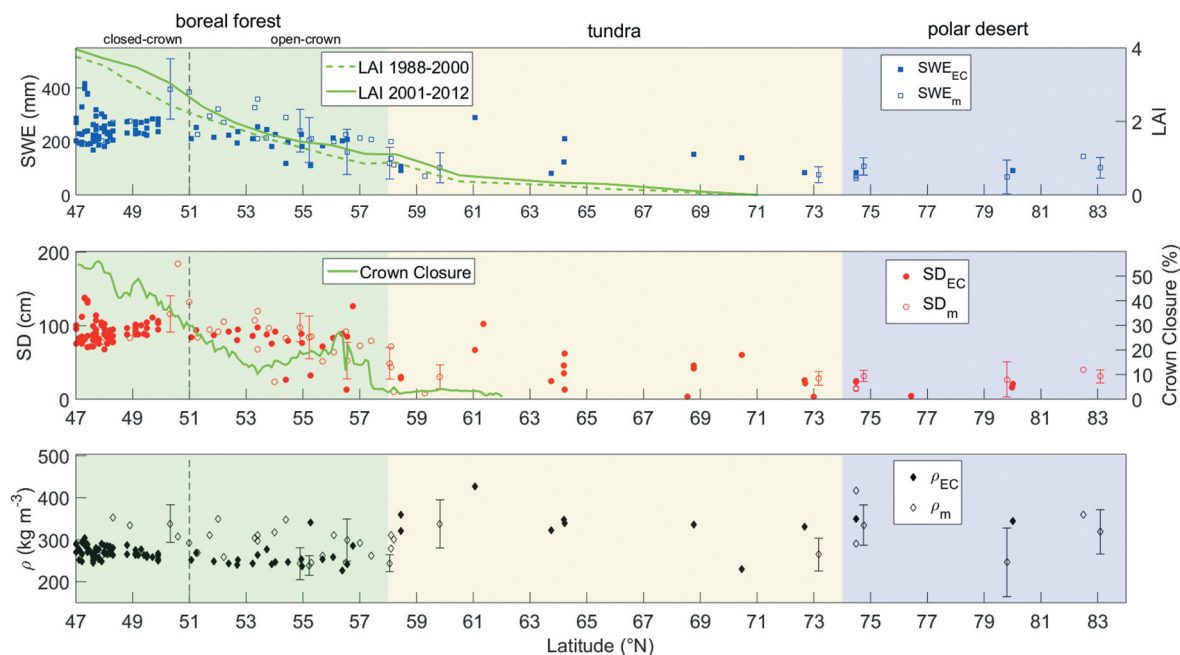

Figure 3. Observational evidence of latitudinal changes in snow cover and vegetation properties over the northeastern Canadian transect studied from 47°N to 83°N. Filled symbols (EC subscript) are from meteorological data and open symbols are from in-situ measurements (m subscript) (field campaigns), all for the period near to the snow maximum (SWE max). Top: snow water equivalent, SWE (mm) (blue symbols); middle: snow depth, SD (cm) (red symbols); bottom: mean (bulk) density (ρ, kg m^{-3}) (black symbols). In top figure, snow data are matched to continuous satellite-derived leaf area index (LAI): averaged LAI for the 1988–2000 period (dotted green line), and for 2001–2012 period (thick green line) (right scale in upper figure). In middle figure, snow data are matched to satellite-derived crown-closure (CC, %) (summer 2011 images). Vertical bars show the ranges of local spatial variability (± standard deviation) over field campaign sites. Background colors separate the three snow-vegetation classes defined in this study (see below and Table 2) and the dotted vertical line delimits the open- from closed-crown boreal forest sub-classes. Table 1 gives the data sources, and Figure 1A shows the site locations.

of SWE at 0.39 indicates the strong local heterogeneity of snow properties, highlighting the well-known difficulty in characterizing snow cover at the local scale (Derksen et al. 2010, 2014).

Figure 3 also shows the LAI and the forest crown-closure fraction (CC) variations along the transect. LAI values decrease from 3.9 at 47°N to 1.1 at 58°N and rapidly drop to almost 0 north of 60°N. The CC parameter, possibly a more robust parameter to characterize dense forest areas, confirms the trend, with a quasi-linear decrease from 54% to 12% between 47°N and 53°N. An increase in CC up to 20% can be observed at 55–57°N, followed by a drastic drop after 57°N (Figure 3). This increase can be related to the forest-tundra ecosystem area that encompasses the transect between 55°N and 57°N (Class 4 in Figure 1(b)) (see also the map in Girard et al. 2008; their Figure 2). The observed CC increase between 55°N and 57°N corresponds exactly to the latitudinal variation of the Forest Tundra Ratio, defined as the forest cover (percentage) per unit area, analyzed by Payette et al. (2001). The CC values at those latitudes are slightly higher than those of the open-crown forest (52°N to 55°N), which would explain these variations (Girard et al. 2008; Leboeuf et al. 2018).

Note that in Figure 3 (top), we also show the temporal evolution of LAI, given for two periods averaged over 1988–2000 and 2001–2012. The evidence of warming on vegetation is clear where mean LAI values increase by 30% from the 1988 to 2000 and 2001 to 2012 periods. The most important increase can be seen around 50°N, at the northern limit of vegetation class 2 (closed-crown

forest) and for vegetation class 4 between 55°N and 57°N, in agreement with Ju and Masek (2016).

Snow classification

The values of the three snowpack parameters (SWE, SD and density) shown in Figure 3 were analyzed in terms of their mean and variability (standard deviation) as a function of latitude over the studied transect in order to propose a classification. It is also based on expert knowledge such as snowpack stratigraphic and microstructural parameters, including density and SSA profiles, and knowledge of the bio-climatic environment. Despite the observed large regional variability, the results show that clusters with a relative consistency in snow properties can effectively be defined within three ranges of latitudes. The data grouped in the ranges 47–58°N, 58–74°N and over 74° show three distinct classes of snowpack, which can be defined as (1) boreal forest snow; (2) tundra snow; (3) and polar desert snow (Figure 4). The boreal forest snow class (47–58°N) encompasses vegetation cover classes 1 to 4 and extends up to the tree line, as far north as Kuujjuaq (see Figure 1(b)). The tundra snow class (58–74°N), which corresponds to vegetation classes 5 to 7, extends past Québec's far north to encompass all of Baffin Island and Bylot Island. The polar desert snow class (74–83°N), i.e., vegetation class 8, covers the northeastern part of the Canadian Arctic Archipelago (Figure 1(b)).

We have compared this classification with the one generated by a purely statistical clustering method. We
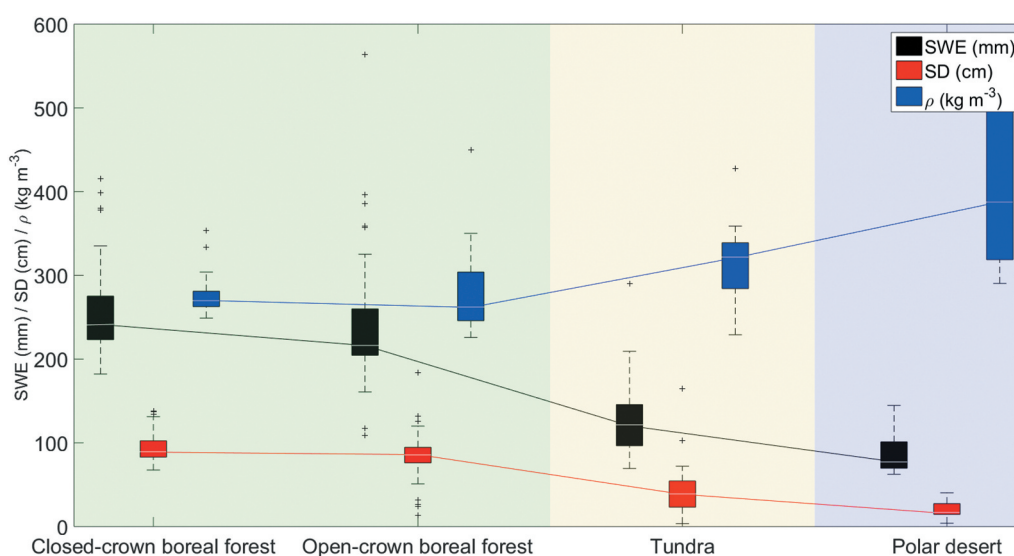

Figure 4. Box plot of Snow Water Equivalent (SWE), Snow Depth (SD) and density (ρ) for each of the three snow classes determined in this study and represented with different colors. Data for closed- and open-crown boreal forest are shown separately to demonstrate that the snowpacks of these two forest classes are not significantly different.

used a density-based approach (DBSCAN, MATLAB® statistical module) to find arbitrarily shaped clusters only driven by a given threshold for the neighborhood search radius in the data triplets (SD, D, SWE) and without setting a number of clusters a priori. In this 3D space, the DBSCAN classification led to the same three classes (boreal, tundra and polar desert), except for 7% misclassified points. These can be clearly replaced by taking into account climatological parameters. This confirms the appropriateness of the three classes initially defined.

The main characteristics of these three classes are described below, and their typical mean and range of parameters (SWE, SD and density) are summarized in Table 2 and Figure 4. The mean climatology of these classes is given in Table 3.

(1) *Boreal forest snow* (47–58°N): Typically includes relatively cold and deep snow covers, up to 250 cm thick, formed by large precipitation amounts (Figure 2). The increased alternation between warm spells and cold temperature observed under current warming leads to the formation of melt features, such as melt-freeze crusts, ice layers and percolation structures in the snowpack. The low wind speed in the forests

does not favor wind slab formation. The snowpack is mostly composed of moderately consolidated fine-grained snow. Due to its high thickness, the insulation properties of this type of snowpack are often good, commonly leading to unfrozen soil throughout the whole winter, with a well-developed depth hoar layer at its base. Layers of faceted crystals form over tens of cm above the basal depth hoar layer. Typical properties of this snow class are close to those of the taiga class from Sturm et al. (1995), although here SD is usually much greater because of the high amount of solid precipitation (Figure 2).

(2) *Tundra snow* (58–74°N): Generally thin snowpack, 20 to 50 cm in depth, in a windy and very cold environment (Figure 1 and Table 3). The ground commonly freezes in early to late fall. The snowpack is typically characterized by an important depth hoar development, with crystals up to a few centimeters long (Domine et al. 2016b). Between the basal depth hoar and the top wind slab, a layer of faceted crystals 1 to 2 mm in size is often observed. This is in fact the initial stage of increased depth hoar layer development (Domine et al. 2016a; Derksen et al. 2014). Furthermore,

Table 2. Proposed snow-vegetation classes over the northeastern Canadian transect. For each class, mean values (standard deviation, Std) of Snow Water Equivalent (SWE), Snow Depth (SD) and density (ρ) are given.

Proposed snow-vegetation classification					Sturm et al.'s (1995) classification	
		Main characteristics				
Latitude	Classes	SWE (±Std) mm	SD (±Std) cm	ρ(±Std) kg m^{-3}	Latitude	Classes
47–58°N	Closed- and open-crown boreal forest snow	250.0 (65.9)	89.8 (22.9)	275.2 (31.5)	<50°N 50–56°N	Maritime Taiga
58–74°N	Herbaceous and low shrub tundra snow	132.9 (57.6)	43.1 (35.2)	315.3 (49.1)	56–82°N	Tundra
74–83°N	Polar desert snow	88.8 (30.5)	19.9 (11.4)	408.6 (106.5)		

Table 3. Measured mean climate variables (and standard deviation, Std) per snow class along the transect: winter (DJFM) air temperature, total snowfall per year and Total Wind Index for wind speed at 10 m height above 6 m s^{-1}. Note that for the boreal forest class, the effective wind speed that impacts snow at the gound level is practically nil.

Snow Class	Latitude range (°N)	Mean Winter Temp. (°C) (Std)	Total snowfall per year (mm w.e.) (Std)	Mean TWI (6 m/s) (Std)
Class 1 Boreal forest	47–58	−16.4 (3.3)	204 (64)	0 * 1266 (604)
Class 2 Tundra	58–74	−23.6 (3.3)	68 (52)	1703 (801)
Class 3 Polar desert	74–83	−31.3 (3.1)	41 (19)	1960** (289) 274 (228)
				xxxx

* At ground level, TWI is null because under the trees.
** Mean value for Resolute Bay (74.75°N).

over the southern boundary zone of this class, warm spells as well as Rain-on-Snow events can take place, leading to the formation of melt-freeze crusts and associated percolation structures within the snowpack (Roy et al. 2016; Langlois et al. 2017; Barrere et al. 2018). The impacts of herbaceous and shrub cover on this snow class are discussed below.

(3) *Polar desert snow* (74–83°N): A thin, very cold and wind-packed snow cover that rarely exceeds 30 cm in height over flat areas. The snowpack typically consists of a basal layer of depth hoar 5 to 10 cm thick overlaid by a thicker hard wind slab (Domine et al. 2002, 2018). However, the formation of depth hoar is particularly modulated by soil moisture availability and wind conditions. Under low soil moisture and high wind conditions in early fall that delay the establishment of a continuous snow cover, the formation of depth hoar can be impeded because the lack of snow cover and soil moisture allow very rapid soil freezing, which limits the temperature gradient in the snowpack. Moreover, snow hardening by wind impedes the water vapor flux, to the point where depth hoar can be totally absent (Domine et al. 2018). The snowpack then has poor thermal insulation properties (typically a snow heat conductivity between 0.05 and 0.2 W m^{-1} K^{-1}, Domine et al. 2007, 2015, 2018, 2019) and ground cooling is enhanced.

The boreal forest snow has high SD and SWE values but relatively low mean density; the tundra snow has lower SD and SWE but higher density, while the polar snow has lower SD and SWE but very high density. This is consistent with the variations in snowfall along the transect, decreasing towards the north (Table 3), shown in Figure 2, and with the wind variations discussed below (Section on the role of wind in snowpack structure). The values of these parameters (SWE, SD and ρ) for each snow class are given in Table 2 and synthesized with box plots in Figure 4. The three classes are statistically different at the 95% confidence level. All differences between parameters of each class show p-values below 0.056 (Student test for differentiating two populations). The differences between the proposed snow classes and those of Sturm et al. (1995) given in Table 2 are addressed in the discussion.

Impact of vegetation on snowpack structure

Results from Figures 3 and 4 show that the snowpack properties are strongly linked to the vegetation types.

When vegetation zones are aggregated into three main classes, i.e., boreal forest, tundra and polar desert, it appears that the observed clusters in snow properties described in the previous section show significant statistical differences.

In Figure 4, typical SWE values of the boreal snow class are significantly different from those in the tundra class. The boreal SWE values range from 200 to 300 mm, with an SD of about twice what can be found in the tundra snow class. We tested whether the type of boreal forest, i.e., closed-crown or open-crown, affected the snowpack variables investigated here. The comparison between closed-crown (<51°N) and open-crown (>51°N) snow classes does not show significant differences, even if closed-crown SD is slightly higher than open-crown SD (93.4 ± 16 cm and 84.1 ± 29 cm, respectively, p = 0.056) (Figure 4). This is likely related to higher precipitation as shown in Figure 2 and Table 3. Because we found that the values of SWE and ρ were not statistically different for these two forest types, they have been grouped together in Table 2.

The vegetation in the tundra zone can be comprised of shrubs 25 to 100 cm tall. The shrubs trap snow leading to higher SD values than on herb tundra. The shrub-covered areas are known to induce increased depth hoar development due to the combination of a strong temperature gradient within the snowpack, high soil moisture and wind protection (Sturm et al. 2001; Domine et al. 2016b). Based on our measured snow profile properties (stratigraphy, density, grain size, SSA) along the transect, the basal depth hoar fraction (DHF) variation is analyzed in Figure 5 and typical SSA profiles for each snow class are presented in the next section (Figure 6).

In Figure 5, the basal depth hoar fraction (DHF) variation with latitude shows that snowpits with erect vegetation (red points), i.e., identified with shrubs at least 10 cm in height in the snowpack, are well distinct from those without erect vegetation (blue points), i.e., with herb, lichen and/or moss covers. The mean DHF value for snowpits with vegetation, 0.63 ± 0.11, is significantly higher than for snowpits without vegetation, 0.40 ± 0.09 (p = 0.0002). Interestingly, the maximum difference in DHF occurs around 56–59°N (Figure 5), where snow density is lower and temperatures are higher than at higher latitudes. Further north at the upper limit of the tundra snow class (72–74°N), the impact of shrubs on DHF is stronger, probably because DH can develop more easily in a thin snowpack whose whole height is affected by shrubs. Depth hoar crystal can then reach 30 mm in size. Snowpack on herb tundra is also characterized by the presence of basal depth hoar, even in windy conditions, due to the increased
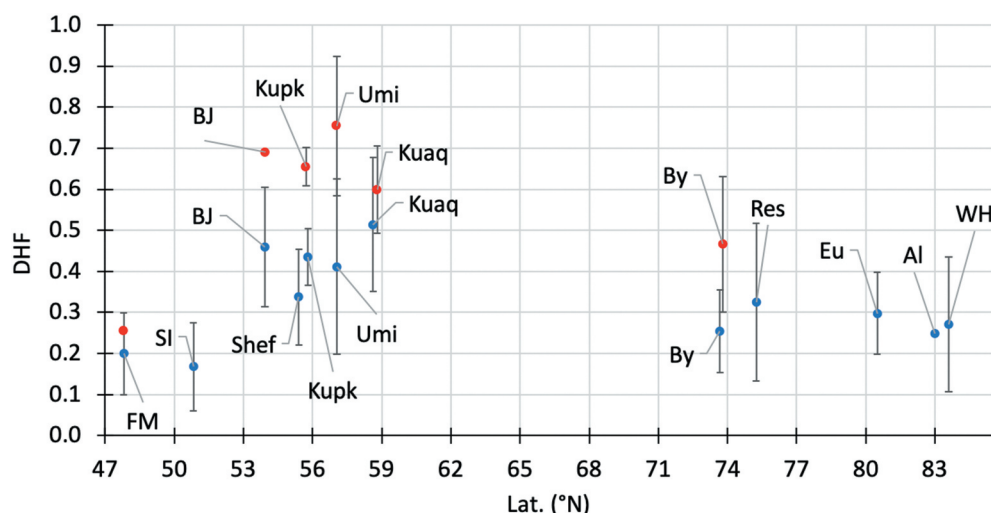
Figure 5. Depth hoar fraction (DHF) (depth hoar thickness over snow depth) along the studied transect. Red points correspond to measurements at sites with shrubs and blue points are for sites without shrubs. The vertical bars show the spatial and/or temporal variability (standard deviation) for each site. See Table 1 for site acronyms.

amount of available soil moisture which delays soil freezing. This strengthens the temperature gradient in the snowpack, providing favorable conditions for depth hoar formation for several months. The observed strong impact of shrubs on basal depth hoar development is in agreement with previous studies such as those described in detail by Sturm et al. (2001) in Alaska (69° N/149°W) and Domine et al. (2016b) on Bylot Island (73° N/80°W).

The main characteristic of the shallow polar desert snow (>74°N) is its very high density, with mean values close to 400 kg m^{-3}. With no erect vegetation and a very low plant cover (~5 to 10%) of low stature vegetation, generally <5 cm tall, snow cover is mainly driven by micro-topography (Derksen et al. 2014) and wind, which can lead to thick and hard wind slabs on exposed surfaces. The depth hoar fraction over the mean 20 ± 11 cm snow depth is of ~0.3, with a strong variability. It strongly depends upon the soil moisture availability, i.e., the type of soil and sparse vegetation. Wind variations along the transect are presented and discussed in the section on the role of wind in snowpack structure.

Snow specific surface area relationships with the snow classification

Snow microstructure is another relevant variable to characterize a snowpack, as it complements density and grain type. We analyzed its variations using an objective descriptor, the surface specific area (SSA), because its vertical distribution and time evolution are very sensitive to meteorological conditions

(Taillandier et al. 2007). SSA data are not as numerous as other variables investigated here because rapid field methods are available only since the development of optical methods (Gallet et al. 2009). As a preliminary investigation, we present in Figure 6 what may be considered representative SSA profiles for each snow class.

For all profiles, SSA decreases with depth. This is expected since SSA decreases over time through metamorphism (both kinetic and equilibrium metamorphism decrease the surface to volume ratio), while higher values can be expected near the air–snow interface from recent precipitation (Taillandier et al. 2007). However, a striking difference is that in the boreal forest snow class, SSA decreases fairly regularly with depth with sometimes different slopes. But in all cases, the boreal class differs clearly from both the tundra and the polar desert classes featuring two distinct layers: a lower depth hoar layer with low SSA and a top wind slab with higher SSA (Domine et al. 2002; Cabanes et al. 2002; Domine et al. 2015, 2016a, 2016b, 2018; Vargel et al. 2020). The upper part of the snowpack has small grain size, SSA from 30 to 60 m^2 kg^{-1}, while the lower layer shows a remarkably constant SSA value around 10 m^2 kg^{-1}. This is the typical structure of Arctic snowpacks, where depth hoar most often has an SSA below 15 m^2 kg^{-1} (Domine et al. 2012, 2016b, 2018). The effects of shrubs appear clearly on these profiles (dotted lines in Figure 6) with lower SSA (larger grain size) than for sites without shrubs (continuous lines) with larger SSA (smaller grain size).
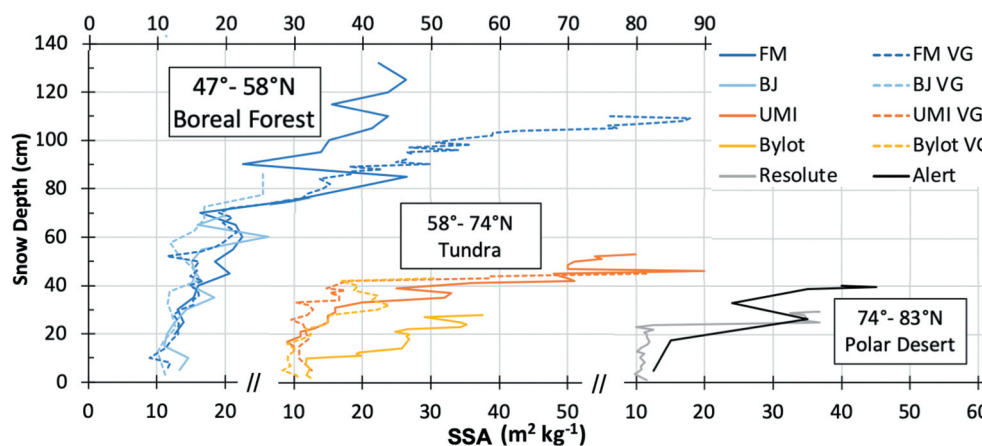
Figure 6. Surface specific area (SSA) profiles (m² kg⁻¹) of each snow class. Continuous lines correspond to sites without erect shrubs and dotted lines (VG) with erect shrubs. See Table 1 for site acronyms. The abscissa is discontinuous for each class, with the same scale, to allow more clarity.

The role of wind in snowpack structure and classification

Along with the temperature gradient in the snowpack, wind is certainly the most important physical variable that affects northern snowpack structure and therefore our classification. In the boreal forest, snow is sheltered from wind and does not directly affect snow density. In tundra and polar desert, wind above about 6 m s⁻¹ causes shear stress on the surface that generates snow particle motion (creeping) and compaction on the surface. This leads to the formation of snow crusts and slabs, whose hardness increases with wind speed (Pomeroy and Brun 2001; Schweizer 2003; Filhol and Sturm 2015; Wright et al. 2018; Sommer et al. 2018).

To characterize the wind effects, we considered the cumulative hourly wind speed above which wind can compact the snow per winter, noted Total Wind Index, TWI, expressed as $\sum_{DJFM} (W - T)$ where the hourly wind speed W is in m s⁻¹ and T is a fixed threshold = 6 m s⁻¹ (inspired from degree-day, see Filhol and Sturm 2015; Domine et al. 2018). The WTI can be seen as a metric for estimating the cumulated energy available to generate wind slabs during the winter along the transect without considering variations in temperature and snow accumulation that can affect snow density (Pomeroy and Brun 2001; Schweizer 2003). Table 3 gives the mean TWI measured at 10 m height for each snow class over the last 20 years of data (data sources: Environment Canada and Nordicana 2020) (Table 3).

Between 58° and 74°N, over the tundra snow class with high TWI (Table 3) and denser snowpacks with lower SD and SWE further north (Figures 3 and 4), no clear relationship appears between TWI and density. Within the polar desert above 75°N, the observed mean TWI for the extreme High Arctic zone, of the order of 274 ± 228, is significantly lower than for the tundra class (Table 3), while the snow density exhibits the highest values. The main factor is that precipitation is 1.7 times lower in the High Arctic than over lower latitudes (see Figure 2). We illustrate the wind–density relationship in more detail within the desert polar class in Figure 7 by considering the interannual density variation, site by site. The results show that the density variation in the top 50% of the snowpack, mainly the wind-packed layer, increases with the cumulated wind speed Index (TWI). The observed relative variability of density below 1000 TWI, with a mean density of 333 ± 49 kg m⁻³, is significantly lower than the density above 1500 TWI, with a mean density of 383 ± 41 kg m⁻³ (p = 1.5E-05). This expected general trend between wind and density thus enriches the specificity of
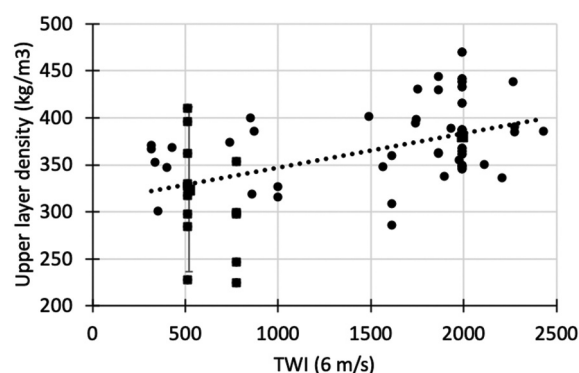

Figure 7. Relationship between the density of the upper layer (top 50% of snowpack) as a function of the Total Wind Index (TWI) above 6 m s⁻¹, at sampled sites in the polar desert snow class: Ward Hunt (83°N), Alert (82.5°N), Eureka (80°N) and Resolute Bay (74.75°N). The vertical bar shows the local spatial variability when the number of snowpits >10. The dotted line is the linear regression (R² = 0.246 and p = 3.7E-05).

the proposed polar desert snow class, in comparison to the first two classes, boreal forest and tundra. However, analyzing this variability individually for each strong wind event throughout the winter is recommended.

In conclusion, the observed snowpack properties (SWE, SD, ρ, DHF and SSA) along the studied transect clearly confirm the rationale for the proposed classification related to climate-vegetation gradient. This finding is particularly important in the context of the observed current shrub expansion, as basal depth hoar layer, linked to shrubs, generally acts as a more insulating layer, reducing ground winter cooling. The specificity of the proposed new polar desert class is also well characterized by a strong wind packing effect, generating a very contrasted SSA profile between a surface wind slab layer over a basal hoar depth layer.

Discussion

Comparison to Sturm et al.'s (1995) classification

The proposed new snow classification for northeastern Canada differs in some respects from that of Sturm et al. (1995) (hereafter S95). S95 proposed a classification system for global seasonal snow covers based on both microstructural-stratigraphic snowpack characteristics and climate variables (wind, precipitation and air temperature). This resulted in six snow classes (tundra, taiga, alpine, maritime, prairie and ephemeral) mapped on a 0.5° latitude × 0.5° longitude grid. Table 2 compares the main differences between S95 and the proposed classification at a regional scale, which considers the vegetation. The S95 classes for the studied transect are mapped in Figure 8, leaving to appear some quasi punctual classes because of the climatic considerations taken into account for small particular areas. The closed- and open-crown boreal forest snow class encompasses two S95 classes: Maritime snow for the southern part (<50°N) and Taiga snow for the northern part. The specificity of northeastern Canada is the combination of high winter precipitation and cold temperatures for the considered latitude (Vincent et al. 2015). The high precipitation over the boreal snow class implies a thicker snowpack and a lower DH fraction than what is described in Sturm's Taiga class. The low temperatures (Figure 2, Table 3) imply that at the southern limit of our area, DH can form quickly and that melting events are less frequent than what is observed in Sturm's Maritime class. Therefore, both these Sturm's classes can be merged in northeastern Canada. The Tundra

snow we define over 58°<Lat.<74°N is similar to the southern part of S95 Tundra snow.

The most important distinction in the snow classification is the proposed introduction of the Polar desert snow class in the High Arctic, which is not considered in the S95 classification (Table 2; Figure 8). Here, we separate the Tundra class of S95 into two classes by considering the specificity of the Polar desert class with higher density, lower SWE and lower SD (see Figure 4) than the mean characteristics of the S95 Tundra class, which is typified by the snow cover in Arctic Alaska.

Climate change and vegetation cover evolution

Although the data collected on snow span a relatively long period of time (2000–2019), we hypothesize that the observed climate change over the past 20 years did not have a direct impact on the physical properties of the snowpack governing our classification. Warming,
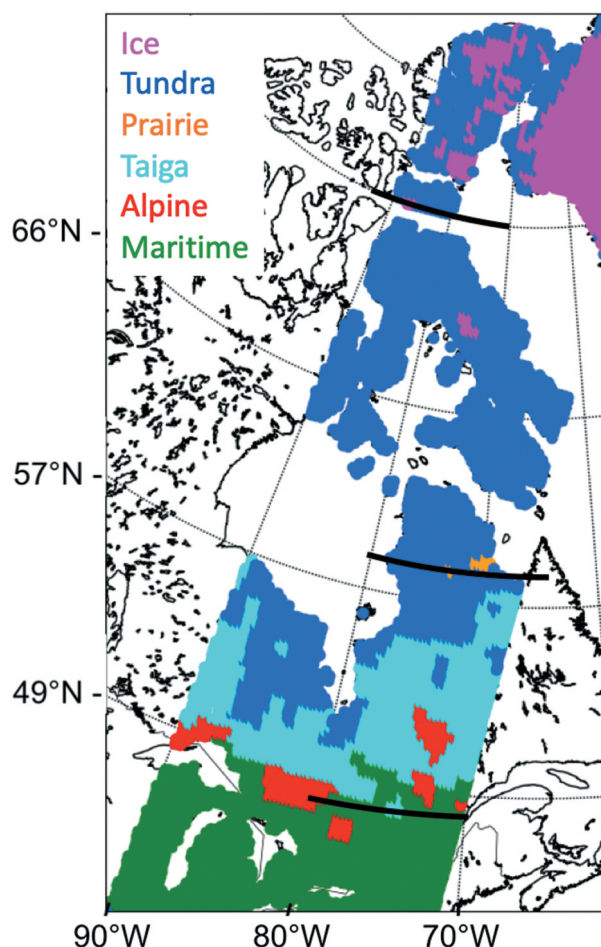

Figure 8. Sturm et al.' (1995) snow classification over the studied transect. The latitudinal limits of the proposed classification (Table 2) are shown (black lines). Sturm et al.'s snow classes include Ice, Tundra, Prairie, Taiga, Alpine and Maritime.

which has been less intense in northeastern than in northwestern Canada (Vincent et al. 2015), leads to significantly smaller changes in temperature when compared to the gradient identified in each zone (Figure 2). Furthermore, the currently observed warming in the North essentially alters snow cover extent and duration, as well as melt onset timing (Vincent et al. 2015; Mudryk et al. 2018). The measured changes in snowfall in the northeast of Canada (above 55°N) (Vincent and Merkis 2006) were not sufficient to modify the snowpack properties at a given location, as observed at sites where data were collected for this study. Until now, rain-on-snow events mainly affect transition periods (fall and spring) (Dolant et al. 2017). Hence, the main climatic factor that could directly affect the snowpack properties used in the classification is wind, which has not evolved significantly over the past two decades. As such, no significant trend was observed in hourly mean wind speed over the 1954–2020 period from meteorological data in the study area (not shown). This result is in agreement with reanalysis datasets, even if large uncertainties exist in the estimated trends of wind speed (Torralba et al. 2017).

We demonstrated in this article that one of the main climatic factors that impact snowpack properties is the indirect effect of the presence/absence of shrubs. However, vegetation responds slowly to climate change. Across northern regions (>50° N), the average velocity of change in growing-season normalized difference vegetation index ('greening index') was less than nearly half of the growing-season mean temperature velocity (Huang et al. 2017). Gagnon et al. (2019) observed that the smallest shrubs that could be sampled on expanding shrub tundra were at least 25 years old, illustrating that the shrub expansion rate is very low. Moreover, the 'Arctic greening' does not necessarily entail an increase in the areal extent of vegetation (Myers-Smith et al. 2020). Numerous studies report that the polar desert vegetation has not changed much over the last 20 years (e.g., Ju and Masek 2016; Meredith et al. 2019; Myers-Smith et al. 2020). Therefore, warming over the course of our study is insufficient to have affected our classification, and the fact that our measurements are spread over 20 years did not alter the analysis presented.

Impacts of snow property changes on ground temperature

Lastly, in the area studied, the continuous permafrost zone spreads northwards from the southern limit of the Tundra snow class at about 57.5°N (Figure 1(a)). Permafrost linked to the ground thermal regime determines major variations in hydrological and nutritional status of soil conditions, and thus drives vegetation distribution and growth. In turn, snow cover and interactions with vegetation modify ground surface temperature.

In the context of northern warming, the variations of the snow cover state during the winter must be considered. In addtion to snowpack physical properties, the net effect of snow on ground temperature depends upon the time of year of snow onset and melt, and snow cover duration. Several studies show that both snow timing and shrub expansion impacts can lead to both ground cooling and ground warming (Ling and Zhang 2003; Bartlett et al. 2004; Zhang 2005). Snow–ground interface temperature records in Alaska from Sturm et al. (1995) confirm the large, up to 10°C, persistent differences in winter soil temperature between shrub and nonshrub sites. Bartlett et al. (2004) show that variation of the duration of the fully insulating snow cover can increase the annual ground temperature by 2–7°C. Frost et al. (2018) report that in Siberia, mature shrubs cooled soils during summer compared to open tundra, but warmed soils by the same intensity (~10°C) in winter, presumably because they developed highly insulative snowpacks. The insulation effect of snow cover can also be counterbalanced by Rain-on-Snow (ROS) (Langlois et al. 2017) and ice crust development following warm spells (Barrere et al. 2018). As these processes are not well modeled in land surface models, they could lead to large uncertainties in the annual ground heat balance with a possibly positive or negative impact on permafrost evolution and therefore on climate because of the feedback related to the carbon cycle in northern regions (Gouttevin et al. 2012; Schuur et al. 2015; Gasser et al. 2018; Biskaborn et al. 2019).

However, globally, with future warming, the snowpack is expected to diminish, enhancing permafrost warming (see Sospedra-Alfonso and William 2017). On the other hand, the snow impact is going to be further strengthened by vegetation growth (Meredith et al. 2019), which leads to a greater proportion of depth hoar (Figure 5), increasing snowpack insulation. Both these factors might lead to enhanced melt of permafrost and related carbon feedbacks.

Conclusion

This study synthesizes the snowpack properties, snow water equivalent, snow depth, density, SSA profiles and basal depth hoar fraction, analyzed along a transect across a region of northeastern Canada between 47°N and 83°N. This unique database was generated from in-situ snow measurements archived over about 20 years of snow research projects, supplemented with all available snow-cover data from weather stations in this region.

A classification of three snow classes along the latitudinal gradient emerges, driven by climate conditions, which control the types of vegetation from boreal forest, tundra and polar desert. Defining worldwide snow classes as in Sturm et al. (1995) (S95) is convenient for many applications, but its use for specific regions can be delicate. We show here that northeastern Canada snow classes are significantly different from those from S95. First, as this study identifies, northeastern Canada features the northernmost seasonal snowpack. Second, precipitation is abundant in the southern part of northeastern Canada and this leads to the definition of the boreal forest type, different from the S95 Taiga class and somewhat overlapping its Maritime class. We also proposed a new snow class, specific to the polar desert region, above 74°N.

Observed changes in snowpack properties along the transect arise from the strong land surface processes generated by the vegetation cover. In particular, we observed that shrubs significantly modify the snow microstructure. In the latitude range of 54° to 74°N, we show that the mean relative depth hoar thickness is significantly higher (57.5%) in shrub areas compared to non-shrub areas. The combined use of satellite remote sensing data on snow and vegetation land cover (Larue et al. 2017; Martin et al. 2017; Pulliainen et al. 2020) can improve future trends of snow–vegetation interactions. The effect of snow cover in the context of climate changes with shrub expansion at the expense of herbaceous or lichen tundra is expected to strengthen snow insulation effects. Our snow classification therefore suggests that snowpack structure could positively feedback on permafrost warming.

Our database is available at http://www.cen.ulaval.ca/nordicanad/dpage.aspx?doi=45705CE-98FC517D461E4C25

Royer A, Domine F, Roy A, Langlois A, Davesne G. 2021. Snowpack physical properties along a transect from 47° to 83°N in northeastern Canada v. 1.0 (2000-2019). Nordicana D87, doi: 10.5885/45705CE-98FC517D461E4C25.

References

AMAP. 2019. AMAP climate change update 2019: an update to key findings of snow, water, ice and permafrost in the Arctic (SWIPA) 2017. Oslo (Norway): Arctic Monitoring and Assessment Programme (AMAP); p. 12.

Barrere M, Domine F, Belke-Brea M, Sarrazin D. 2018. Snowmelt events in autumn can reduce or cancel the soil warming effect of snow–vegetation interactions in the Arctic. J Climate. 3:9507–9518. doi:10.1175/JCLI-D-18-0135.1.

Barrere M, Domine F, Decharme B, Morin S, Vionnet V, Lafaysse M. 2017. Evaluating the performance of coupled snow–soil models in SURFEXv8 to simulate the permafrost thermal regime at a high Arctic site. Geosci Model Dev. 10 (9):3461–3479. doi:10.5194/gmd-10-3461-2017.

Bartlett G, Chapman DS, Harris RN. 2004. Snow and the ground temperature record of climate change. J Geophys Res. 109. doi:10.1029/2004JF000224.

Beaudoin A, Bernier PY, Villemaire P, Guindon L, Guo XJ. 2017a. Tracking forest attributes across Canada between 2001 and 2011 using a kNN mapping approach applied to MODIS imagery. Can J Forest Res. 48:85–93. doi:10.1139/cjfr-2017-0184.

Beaudoin A, Bernier PY, Villemaire P, Guindon L, Guo XJ. 2017b. Species composition, forest properties and land cover types across Canada's forests at 250m resolution for 2001 and 2011. Québec (Canada): Natural Resources Canada, Canadian Forest Service, Laurentian Forestry Centre. doi:10.23687/ec9e2659-1c29-4ddb-87a2-6aced147a990.

Biskaborn BK, Smith SL, Noetzli J, Matthes H, Vieira G, Streletskiy DA, Schoeneich P, Romanovsky VE, Lewkowicz AG, Abramov A, et al. 2019. Permafrost is

warming at a global scale. Nat Commun 10:264. doi:10.1038/s41467-018-08240-4.

Bliss LC, Matveyeva NV. 1992. Circumpolar Arctic vegetation. In: Chapin III FS, Jefferies RL, Reynolds JF, Shaver GR, Svoboda J, editors. Arctic ecosystems in a changing climate: an ecophysiological perspective. San Diego (California, USA): Academic Press; p. 59–89.

Bokhorst S, Pedersen S, Brucker L, Anisimov O, Bjerke J, Brown R, Ehrich D, Essery R, Heilig A, Ingvander S, et al. 2016. Changing Arctic snow cover: a review of recent developments and assessment of future needs for observations, modelling, and impacts. Ambio. 45(5):516–537. doi:10.1007/s13280-016-0770-0.

Brown R, Derksen C, Wang L. 2010. A multi-dataset analysis of variability and change in Arctic spring snow cover extent, 1967–2008. J Geophys Res. 115:D16111. doi:10.1029/2010JD013975.

Brown R, Fang B, Mudryk L. 2019. Update of Canadian historical snow survey data and analysis of snow water equivalent trends, 1967–2016. Atmosphere-Ocean. 57(2):149–156. doi:10.1080/07055900.2019.1598843.

Brown RD, Mote P. 2009. The response of Northern Hemisphere snow cover to a changing climate. J Climate. 22:2124–2145. doi:10.1175/2008JCLI2665.1.

Busseau BC, Royer A, Langlois A, Domine F. 2017. Analysis of snow-vegetation interactions in the Low Arctic – subarctic transition zone (north-eastern Canada). Physical Geography. 38(2):159–175. doi:10.1080/02723646.2017.1283477.

Cabanes A, Legagneux L, Domine F. 2002. Evolution of the specific surface area and of crystal morphology of Arctic fresh snow during the ALERT 2000 campaign. Atmos Environ. 36:2767–2777. doi:10.1016/S1352-2310(02)00111-5.

Callaghan TV, Tweedie CE, Åkerman J, Andrew C, Bergstedt J, Butler MG, Christensen TR, Cooley D, Dahlberg U, Danby RK, et al. 2011. Multi-decadal changes in tundra environments and ecosystems: synthesis of the International Polar Year - Back to the Future project (IPY-BTF). Ambio. 40:705. doi:10.1007/s13280-011-0179-8.

CAVM. 2003. Circumpolar Arctic Vegetation Map (CAVM) project. (1:7,500,000 scale), Conservation of Arctic Flora and Fauna (CAFF) Map No. 1. Anchorage (Alaska): U.S. Fish and Wildlife Service.

Chadburn SE, Burke EJ, Essery RLH, Boike J, Langer M, Heikenfeld M, Cox PM, Friedlingstein P. 2015. Impact of model developments on present and future simulations of permafrost in a global land-surface model. Cryosphere. 9:1505–1521. doi:10.5194/tc-9-1505-2015.

Colbeck SC. 1993. The vapor diffusion-coefficient for snow. Water Resour Res. 29(1):109–115. doi:10.1029/92WR02301.

Derksen C, Lemmetyinen J, Toose P, Silis A, Pulliainen J, Sturm M. 2014. Physical properties of Arctic versus subarctic snow: implications for high latitude passive microwave snow water equivalent retrievals. J Geophys Res Atmos. 119:7254–7270. doi:10.1002/2013JD021264.

Derksen C, Toose P, Rees A, Wang L, English M, Walker A, Sturm M. 2010. Development of a tundra-specific snow water equivalent retrieval algorithm for satellite passive microwave data. Remote Sens Environ. 114(8):1699–1709. doi:10.1016/j.rse.2010.02.019.

Diro GT, Sushama L. 2020. Contribution of snow cover decline to projected warming over North America. Geophys Res Lett. 47(e2019GL084414). doi:10.1029/2019GL084414.

Dolant C, Langlois A, Brucker L, Royer A, Roy A, Montpetit B. 2017. Meteorological inventory of Rain-On-Snow events in the Canadian Arctic Archipelago and satellite detection assessment using passive microwave data. Phys Geogr. doi:10.1080/02723646.2017.1400339.

Domine F, Barrere M, Morin S. 2016a. The growth of shrubs on high Arctic tundra at Bylot Island: impact on snow physical properties and permafrost thermal regime. Biogeosciences. 13(23):6471–6486. doi:10.5194/bg-13-6471-2016.

Domine F, Barrere M, Sarrazin D. 2016b. Seasonal evolution of the effective thermal conductivity of the snow and the soil in high Arctic herb tundra at Bylot Island, Canada. Cryosphere. 10(6):2573–2588. doi:10.5194/tc-10-2573-2016.

Domine F, Barrere M, Sarrazin D, Morin S, Arnaud L. 2015. Automatic monitoring of the effective thermal conductivity of snow in a low-Arctic shrub tundra. Cryosphere. 9 (3):1265–1276. doi:10.5194/tc-9-1265-2015.

Domine F, Belke-Brea M, Sarrazin D, Arnaud L, Barrere M, Poirier M. 2018. Soil moisture, wind speed and depth hoar formation in the Arctic snowpack. J Glaciol. 64 (248):990–1002. doi:10.1017/jog.2018.89.

Domine F, Cabanes A, Legagneux L. 2002. Structure, microphysics, and surface area of the Arctic snowpack near Alert during the ALERT 2000 campaign. Atmos Environ. 36(15–16):2753–2765. doi:10.1016/S1352-2310(02)00108-5.

Domine F, Picard G, Morin S, Barrere M, Madore J-B, Langlois A. 2019. Major issues in simulating some Arctic snowpack properties using current detailed snow physics models: consequences for the thermal regime and water budget of permafrost. J Adv Model Earth Sys. 11(1):34–44. doi:10.1029/2018MS001445.

Domine F., Taillandier A. S., Simpson W. R. 2007. A parameterization of the specific surface area of seasonal snow for field use and for models of snowpack evolution. J. Geophys. Res. 112(F02031):13.

Dutra E, Viterbo P, Miranda PMA, Balsamo G. 2012. Complexity of snow schemes in a climate model and its impact on surface energy and hydrology. J Hydrometeorol. 13 (2):521–538. doi:10.1175/JHM-D-11-072.1.

Fierz C, Armstrong RL, Duran Y, Etchevers P, Greene E, McClung DM, Nishimura K, Satyawali PK, Sokratov SA. 2009. The international classification for seasonal snow on the ground. IHP-VII technical documents in hydrology N°83, IACS contribution N°1. Paris: UNESCO-IHP.

Filhol S, Sturm S. 2015. Snow bedforms: a review, new data, and a formation model. J Geophys Res Earth Surf. 120 (9):1645–1669. doi:10.1002/2015JF003529.

Frost GV, Epstein HE, Walker DA, Matyshack G, Ermokhina K. 2018. Seasonal and long-term changes to Active-layer temperatures after tall shrubland expansion and succession in Arctic tundra. Ecosystems. 21(3):507–520. doi:10.1007/s10021-017-0165-5.

Gagnon M, Domine F, Boudreau S. 2019. The carbon sink due to shrub growth on Arctic tundra: a case study in a carbon-poor soil in eastern Canada. Environ Res Commun. 1(9):091001. doi:10.1088/2515-7620/ab3cdd.

Gallet J, Domine F, Zender C, Picard G. 2009. Measurement of the specific surface area of snow using infrared reflectance in an integrating sphere at 1310 and 1550 nm. Cryosphere. 3 (2):167–182. doi:10.5194/tc-3-167-2009.

Gasser T, Kechiar M, Ciais P, Burke EJ, Kleinen T, Zhu D, Huang Y, Ekici A, Obersteiner M. 2018. Path-dependent reductions in CO_2 emission budgets caused by permafrost carbon release. Nature Geosci. 11(11):830–835. doi:10.1038/s41561-018-0227-0.

Girard F, Payette S, Gagnon R. 2008. Rapid expansion of lichen woodlands within the closed-crown boreal forest zone over the last 50 years caused by stand disturbances in eastern Canada. J Biogeogr. 35(3):529–537. doi:10.1111/j.1365-2699.2007.01816.x.

Gouttevin I, Menegoz M, Domine F, Krinner G, Koven C, Ciais P, Tarnocai C, Boike J. 2012. How the insulating properties of snow affect soil carbon distribution in the continental pan-Arctic area. J Geophys Res. 117:G02020. doi:10.1029/2011JG001916.

Gouttevin I., Langer M., Löwe H., Boike J., Proksch M., Schneebeli M. 2018. Observation and modelling of snow at a polygonal tundra permafrost site: spatial variability and thermal implications. Cryosphere. 12:3693–3717.

Grünberg I, Wilcox EJ, Zwieback S, Marsh P, Boike J. 2020. Linking tundra vegetation, snow, soil temperature, and permafrost. Biogeosciences. 17(16):4261–4279. doi:10.5194/bg-17-4261-2020.

Huang M, Piao S, Janssens I, Zhu Z, Wang T, Wu D, Ciais P, Myneni R, Peaucelle M, Peng S, et al. 2017. Velocity of change in vegetation productivity over northern high latitudes. Nature Ecol Evol. 1(11):1649–1654. doi:10.1038/s41559-017-0328-y.

Ju J, Masek JG. 2016. The vegetation greenness trend in Canada and US Alaska from 1984– 2012 Landsat data. Remote Sens Environ. 176:1–16. doi:10.1016/j.rse.2016.01.001.

Karger DN, Conrad O, Böhner J, Kawohl T, Kreft H, Soria-Auza RW, Zimmermann NE, Linder HP, Kessler M. 2017. Climatologies at high resolution for the earth's land surface areas. Scientific Data. 4(1):170122. doi:10.1038/sdata.2017.122.

Langlois A, Johnson C-A, Montpetit B, Royer A, Blukacz-Richards EA, Neave E, Dolant C, Roy A, Arhonditsis G, Kim D-K, et al. 2017. Detection of rain-on-snow (ROS) events and ice layer formation using passive microwave radiometry: a context for Peary caribou habitat in the Canadian Arctic. Remote Sens Environ. 189:84–95. doi:10.1016/j.rse.2016.11.006.

Langlois A, Royer A, Goïta K. 2010. Analysis of simulated and spaceborne passive microwave brightness temperature using in situ measurements of snow and vegetation properties. Can J Remote Sens. 36(S1):135–148. doi:10.5589/m10-016.

Langlois A, Royer A, Montpetit B, Roy A, Durocher M. 2020. Presenting snow grain size and shape distributions in Northern Canada using a new photographic device allowing 2D and 3D representation of snow grains. Front Earth Sci. 7:347. doi:10.3389/feart.2019.00347.

Larue F, Royer A, De Sève D, Langlois A, Roy A, Brucker B. 2017. Validation of GlobSnow-2 snow water equivalent over Eastern Canada. Remote Sens Environ. 194:264–277. doi:10.1016/j.rse.2017.03.027.

Larue F, Royer A, De Sève D, Roy A, Picard G, Vionnet V. 2018. Simulation and assimilation of passive microwave data using a snowpack model coupled to a calibrated radiative transfer model over North-Eastern Canada. Water Resour Res. 54(7):4823–4848. doi:10.1029/2017WR022132.

Lawrence DM, Slater AG. 2010. The contribution of snow condition trends to future ground climate. Clim Dynam. 34(7-–8):969–981. doi:10.1007/s00382-009-0537-4.

Leboeuf A, Morneau C, Robitaille A, Dufour E, Grondin P. 2018. Ecological mapping of the vegetation of Northern Québec. Québec (QC, Canada): Ministere des Forets, de la Faune et des Parcs.

Ling F, Zhang T. 2003. Impact of the timing and duration of seasonal snow cover on the active layer and permafrost in the Alaskan Arctic. Permafrost Periglac. 14(2):141–150. doi:10.1002/ppp.445.

Liston GE, Hiemstra CA. 2011. The changing cryosphere: Pan-Arctic snow trends (1979–2009). J Climate. 24 (21):5691–5712. doi:10.1175/JCLI-D-11-00081.1.

Marsh P, Bartlett P, MacKay M, Pohl S, Lantz T. 2010. Snowmelt energetics at a shrub tundra site in the western Canadian Arctic. Hydrol Process. 24(25):3603–3620. doi:10.1002/hyp.7786.

Martin AC, Jeffers ES, Petrokofsky G, Myers-Smith I, Macias-Fauria M. 2017. Shrub growth and expansion in the Arctic tundra: an assessment of controlling factors using an evidence-based approach. Environ Res Lett. 12(8):085007. doi:10.1088/1748-9326/aa7989.

Meredith M, Sommerkorn M, Cassotta S, Derksen C, Ekaykin A, Hollowed A, Kofinas G, Mackintosh A, Melbourne-Thomas J, et al. 2019. Polar regions. In: Portner H-O, Roberts DC, Masson-Delmotte V, Zhai P, Tignor M, Poloczanska E, Mintenbeck K, Alegria A, Nicolai M, Okem A et al, editors. IPCC special report on the ocean and cryosphere in a changing climate. Geneva, Switzerland: Intergovernmental Panel on Climate Change. https://www.ipcc.ch/srocc/chapter/chapter-3-2/ .

Montpetit B, Royer A, Langlois A, Cliche P, Roy A, Champollion N, Picard G, Domine F, Obbard R. 2012. New shortwave infrared albedo measurements for snow specific surface area retrieval. J Glaciol. 58(211):941–952. doi:10.3189/2012JoG11J248.

Mortimer C, Mudryk L, Derksen C, Luojus K, Brown R, Kelly R, Tedesco M. 2020. Evaluation of long-term Northern Hemisphere snow water equivalent products. Cryosphere. 14(5):1579–1594. doi:10.5194/tc-14-1579-2020.

Mudryk LR, Derksen C, Howell S, Laliberté F, Thackeray C, Sospedra-Alfonso R, Vionnet V, Kushner PJ, Brown R. 2018. Canadian snow and sea ice: historical trends and projections. Cryosphere. 12(4):1157–1176. doi:10.5194/tc-12-1157-2018.

Myers-Smith IH, Forbes BC, Wilmking M, Hallinger M, Lantz T, Blok D, Tape KD, Macias-Fauria M, Sass-Klaasse U, Lévesque E, et al. 2011. Shrub expansion in tundra ecosystems: dynamics, impacts and research priorities. Environ Res Lett. 48(4):045509. doi:10.1139/cjfr-2017-0184.

Myers-Smith IH, Kerby JT, Phoenix GK, Bjerke JW, Epstein HE, Assmann JJ, John C, Andreu-Hayles L, Angers-Blondin S,

Beck PSA, et al. 2020. Complexity revealed in the greening of the Arctic. Nat Clim Chang. 10(2):106–117. doi:10.1038/s41558-019-0688-1.

Nordicana D. 2020. Meteorological data from the CEN-SILA network in Nunavut and Northern Québec, Canada. Québec (Québec) (Canada): Centre d'études nordiques. http://www.cen.ulaval.ca/nordicanad/ .

Paquin J-P, Sushama L. 2015. On the Arctic near-surface permafrost and climate sensitivities to soil and snow model formulations in climate models. Clim Dynam. 44(1–2):203–228. doi:10.1007/s00382-014-2185-6.

Paradis M, Levesque E, Boudreau S. 2016. Greater effect of increasing shrub height on winter versus summer soil temperature. Environ Res Lett. 11(8):085005. doi:10.1088/1748-9326/11/8/085005.

Park H, Fedorov A, Zheleznyak M, Konstantinov P, Walsh J. 2015. Effect of snow cover on pan-Arctic permafrost thermal regimes. Clim Dynam. 44(9–10):2873–2895. doi:10.1007/s00382-014-2356-5.

Payette S. 1992. Fire as a controlling process in the North American boreal forest. In: Shugart HH, Leemans R, Bonan GB, editors. A systems analysis of the global boreal forest. Cambridge (UK): Cambridge University Press; p. 144–169.

Payette S, Delwaide A. 2018. Tamm review: the North-American lichen woodland. Forest Ecol Manag. 417:167–183. doi:10.1016/j.foreco.2018.02.043.

Payette S, Fortin M-J, Gamache I. 2001. The subarctic forest–tundra: the structure of a biome in a changing climate. BioScience. 51(9):709–718. doi:10.1641/0006-3568(2001)051[0709:TSFTTS]2.0.CO;2.

Pearson RG, Phillips SJ, Loranty MM, Beck PS, Damoulas T, Knight SJ, Goetz SJ. 2013. Shifts in Arctic vegetation and associated feedbacks under climate change. Nat Climate Change. 3(7):673–677. doi:10.1038/nclimate1858.

Pomeroy JW, Brun E. 2001. Physical properties of snow. In: Jones HG, Pomeroy JW, Walker DA, Hoham RW, editors. Snow ecology: an interdisciplinary examination of snow-covered ecosystems. Cambridge (UK): Cambridge University Press; p. 45–126.

Proksch M, Rutter N, Fierz C, Schneebeli M. 2016. Intercomparison of snow density measurements: bias, precision, and vertical resolution. The Cryosphere. 10(1):371–384. doi:10.5194/tc-10-371-2016.

Pulliainen J, Luojus K, Derksen C, Mudryk L, Lemmetyinen J, Salminen M, Ikonen J, Takala M, Cohen J, Smolander T, et al. 2020. Patterns and trends of Northern Hemisphere snow mass from 1980 to 2018. Nature. 581(7808):294–298. doi:10.1038/s41586-020-2258-0.

Roy A, Royer A, St-Jean-Rondeau O, Montpetit B, Picard G, Mavrovic A, Marchand N, Langlois A. 2016. Microwave snow emission modeling uncertainties in boreal and subarctic environments. The Cryosphere. 10(2):623–638. doi:10.5194/tc-10-623-2016.

Saberi N, Kelly R, Toose P, Roy A, Derksen C. 2017. Modeling the observed microwave emission from shallow multi-layer tundra snow using DMRT-ML. Remote Sens. 9(12):1327. doi:10.3390/rs9121327.

Schuur EAG, McGuire AD, Schädel C, Grosse G, Harden JW, Hayes DJ, Hugelius G, Koven CD, Kuhry P, Lawrence DM, et al. 2015. Climate change and the permafrost carbon feedback. Nature. 520(7546):171–179. doi:10.1038/nature14338.

Schweizer J. 2003. Snow avalanche formation. Rev Geophys. 41(4):1016–1041. doi:10.1029/2002RG000123.

Sommer CG, Wever N, Fierz C, Lehning M. 2018. Investigation of a wind-packing event in Queen Maud Land, Antarctica. Cryosphere. 12(9):2923–2939. doi:10.5194/tc-12-2923-2018.

Sospedra-Alfonso R, William M. 2017. Influences of temperature and precipitation on historical and future snowpack variability over the Northern Hemisphere in the Second Generation Canadian Earth System Model. J Climate. 30(12):4633–4656. doi:10.1175/JCLI-D-16-0612.1.

Sturm M, Benson CS. 1997. Vapor transport, grain growth and depth-hoar development in the subarctic snow. J Glaciol. 43(143):42–59. doi:10.1017/S0022143000002793.

Sturm M, Holmgren J, Liston GE. 1995. A seasonal snow cover classification system for local to global applications. J Climate. 8:1261–128. 10.1175/1520-0442(1995)008%3C1261:ASSCCS%3E2.0.CO;2.

Sturm M, Mcfadden JP, Liston GE, ChapinIII FS, Racine CH, Holmgren J. 2001. Snow–shrub interactions in Arctic tundra: a hypothesis with climatic implications. J Climate. 14:336–344. 10.1175/1520-0442(2001)014%3C0336:SSIIAT%3E2.0.CO;2.

Taillandier AS, Domine F, Simpson WR, Sturm M, Douglas TA. 2007. Rate of decrease of the specific surface area of dry snow: isothermal and temperature gradient conditions. J Geophys Res Earth Surf. 112:F03003. doi:10.1029/2006jf000514.

Takala M, Luoju K, Pulliainen J, Derksen C, Lemmetyinen J, Kärnä J-P, Koskinen J, Bojkov B. 2011. Estimating northern hemisphere snow water equivalent for climate research through assimilation of space-borne radiometer data and ground-based measurements. Remote Sens Environ. 115(12):3517–3529. doi:10.1016/j.rse.2011.08.014.

Tape K, Sturm M, Racine C. 2006. The evidence for shrub expansion in northern Alaska and the pan-Arctic. Global Change Biol. 12:686–702. doi:10.1111/j.1365-2486.2006.01128.x.

Torralba V, Doblas-Reyes FJ, Gonzalez-Reviriego N. 2017. Uncertainty in recent near-surface wind speed trends: a global reanalysis intercomparison. Environ Res Lett. 12(11):114019. doi:10.1088/1748-9326/aa8a58.

Vargel V., Royer A., St-Jean-Rondeau O., Picard G., Roy A., Sasseville V., Langlois A. 2020. Arctic and Subarctic snow microstructure analysis for microwave brightness temperature simulations. Remote Sens. Environ. 242:111754.

Vincent L.A., Mekis L. 2006. Changes in daily and extreme temperature and precipitation indices for Canada over the twentieth century. Atmos. Ocean. 44(2):177-193.

Vincent LA, Zhang X, Brown RD, Feng Y, Mekis E, Milewska EJ, Wang H, Wang XL. 2015. Observed trends in Canada's climate and influence of low-frequency variability modes. J Climate. 28(11):4545–4560. doi:10.1175/JCLI-D-14-00697.1.

Wright PJ, Comey B, Comey M. 2018. Thresholds in wind speed, air temperature and relative humidity controlling slab formation. Proceedings, International Snow Science Workshop, Innsbruck, Austria; p. 987–991.

Xiao ZQ, Liang S, Wang J, Xiang Y, Zhao X, Song J. 2016. Long-time-series global land surface satellite leaf area index product derived from MODIS and AVHRR surface reflectance.

IEEE T Geosci Remote. 54(9):5301–5318. doi:10.1109/TGRS.2016.2560522.

Xu L, Myneni RB, Chapin III FS, Callaghan TV, Pinzon JE, Tucker CJ, Zhu Z, Bi J, Ciais P, Tømmervik H, et al. 2013. Temperature and vegetation seasonality diminishment over northern lands. Nature Clim Change. 3:581–586. doi:10.1038/nclimate1836.

Zhang T. 2005. Influence of the seasonal snow cover on the ground thermal regime: an overview. Rev Geophys. 43. doi:10.1029/2004RG000157.

Zhang T, Osterkamp TE, Stamnes K. 1996. Influence of the depth hoar layer of the seasonal snow cover on the ground thermal regime. Water Resour Res. 32:2075–2086. doi:10.1029/96WR00996.